EXPERIMENTAL INVESTIGATION OF THE FLOTATION STABILITY OF A HELICOPTER AFTER DITCHING

Simon Tödter, University of Duisburg-Essen, Institute of Sustainable and Autonomous Maritime Systems, Duisburg, Germany
Jens Neugebauer, University of Duisburg-Essen, Institute of Sustainable and Autonomous Maritime Systems, Duisburg, Germany
Ould el Moctar, University of Duisburg-Essen, Institute of Sustainable and Autonomous Maritime Systems, Duisburg, Germany
Stefan Harms, Airbus Helicopters, Germany
Thomas E. Schellin, University of Duisburg-Essen, Institute of Sustainable and Autonomous Maritime Systems, Duisburg, Germany

Abstract
Recent helicopter accident reviews show that more than 50% of all fatalities after ditching happened due to helicopter capsizing and, consequently, drowning of passengers and crew. In the present study, we experimentally investigated the flotation stability of a modern light helicopter equipped with a state-of-the-art flotation system. We monitored waves and sea spectra, measured helicopter motions and evaluated capsize probabilities for significant wave heights of 5 and 6 m. Resulting capsize probabilities were up to 13.1%. The helicopter was also tested with attached scoops, which did not show a positive effect on capsize probabilities and roll angles. Additionally, the effect of one opened cabin door was studied, which had no effect on the flotation stability.

1. INTRODUCTION

The operation of offshore oil and gas as well as "renewable" energy harvesting requires frequent transfer of crews and maintenance workers. These transfers are usually done by crew transfer vessels. However, the increasing distance between shore and destination makes the utilization of a helicopter favorable for many transfer operations. A possible application of floating offshore wind turbines far away from shore is likely to accelerate this trend. Thus, operational safety becomes more prominent.

Over the time period from 1971 till 1992, 338 fatalities resulted from civil helicopter water impacts (Ref. 1), and 56.7% of these fatalities were caused by drowning. Additionally, for military helicopters of the United Kingdom (UK), 82.6% of all fatalities after ditching were due to drowning. Downie and Gosling (Ref. 2) reviewed accidents of offshore helicopter travel in the UK. The Civil Aviation Authority (Ref. 3) reported that, in the North Sea between 1976 and 2012, 31 out 38 fatalities resulted from drowning. Rowe et al. (Ref. 4), comparing offshore helicopter accidents in the UK and in the Gulf of Mexico between 1995 and 1999, documented an accident rate of 1.74 and 1.40 per 100,000 flying hours, respectively. They also summarized recommendations to increase the safety after ditching. Aziz et al. (Ref. 5) used ditching accidents listed in the SKYbrary to indicate risk factors for ditching. They also documented that 60% of fatalities after ditching resulted from drowning. Furthermore, the Federal Aviation Administration (Ref. 6), reviewing ditching and water-impacts of helicopters in the United States from 1982 through 1989, reported that ten out of twenty post-impact injuries resulted in drowning.

Brooks et al. (Ref. 7) compared in detail the ditching of helicopters registered in Canada. They reported that, of the 46 cases evaluated, at least 21 helicopters capsized and 33 sank. However, the final floating position of the ditched helicopters was not documented in all cases. All accidents took place during daylight hours and, consequently, the 78% survival rate was relatively high. Taber and McCabe (Ref. 8) analyzed 511 helicopter ditching accidents. From the 382 cases for which the final helicopter position was recorded, 85% capsized. They also empathized that simply mounting external floats did not increase the survival rate when these floats were unsuitable or inadequately attached. Nevertheless, capsizing and sinking of the helicopter lowered the survival rate.

The high number of casualties due to drowning in combination with the large rate of capsized helicopters calls for an evolution of flotation systems to increase the safety for passengers and crew during offshore helicopter travel (Ref. 9). Therefore, an analysis of the capability of existing flotation system is necessary. Taber and McCabe (Ref. 8) advocated that traditional float shapes may not suffice to offer a sufficient level of safety.

To decrease the number of fatalities and, respectively, the number of helicopter capsizing events, the European Union Aviation Safety Agency (EASA) introduced new certification guidelines for offshore helicopters (Ref. 10 and 11), which require experimentally investigating the flotation stability and the resulting capsize rate of a helicopter in a sea state modeled by irregular waves. These experiments continue a long history of model-scale helicopter flotation stability experiments. Kidwell and Crago (Ref. 12) investigated a helicopter model floating in regular and irregular waves. They concluded that, for twin-float helicopters, capsizing in regular waves is impossible. Only breaking waves hitting the helicopter in beam seas may capsize the helicopter. Wilson and Tucker (1987), carrying out model-scale experiments for sea states 4, 5, and 6, concluded that the helicopter was unlikely to survive in sea states 5 and 6; however, it would survive sea state 4. Alcedo (Ref. 14) conducted flotation tests in waves of varying steepness. Delorme et al. (Ref. 15) considered irregular waves of sea states 3 and 5 to analyze the functionality of floats attached at the top of a helicopter's fuselage to prevent a its total inversion after capsizing. Kraskowski (Ref. 16) studied experimentally and numerically heave, roll, and pitch motions of a floating helicopter. Additionally, Katsuno et al. (Ret. 17-19) numerically investigated the flotation behavior of a helicopter after ditching.

In our present study, we conducted model-scale experiments in irregular waves representing sea state 6 to quantify the capsizing rate of a modern light helicopter equipped with a state-of-the-art inflatable flotation system.

2. EXPERIMENTAL SETUP

Our experimental setup had to account for the size of the helicopter model relative to the wave basin. For light helicopters, the scale ratio λ should be as small as possible although a large scale factor enables a more realistic adjustment of the helicopter's center of gravity (CoG) and moments of inertia. On the other hand, the wave basin has to be capable to generate waves appropriate to the chosen scale factor. Thus, a larger scale factor and a correspondingly smaller model enable a wider range of feasible test facilities. Additionally, EASA (Ref. 11) specifies that the scale factor must be smaller than fifteen. Consequently, we selected a scale factor of twelve.

2.1. THE HELICOPTER MODEL

Our helicopter model was scaled according to the Froude scaling law. Thus, its length L, width B, and height H_H represented the full-scale helicopter. The model's fuselage and its landing gear were made of carbon fiber, while the floats were milled out of XPS foam. The four removable floats, screwed to the landing gear, allowed investigating different floating configurations. The buoyancy provided by all four floats equaled 148% of the helicopter's greatest mass configuration; the two forward floats supplied 57.3% of its buoyancy. However, depending on the helicopter's floating position, the landing gear and parts of the fuselage also contributed to the helicopter's total buoyancy. Printed scoops were attached to the floats, using adhesive tape for some tests, to investigate their influence on floating stability. The forward and aft scoops had a diameter representing 36.7% of the float diameter and a length representing 50.6% and 51.9% of the forward and aft float lengths, respectively.

The passenger doors of the fuselage, printed out of polylactide, were screwed to the fuselage. Thus, the model also was tested with opened doors to analyze the effect of the flooded fuselage on floating stability. To allow for a realistic flooding of the cabin, the cabin floor was covered by a thin foil to prevent water entered the lower part of the fuselage. The helicopter rotor was not modeled; however, its weight was accounted for. The simply modeled helicopter tail shifted the helicopter's CoG slightly forward. Figure 1 pictures a drawing of the helicopter and a close-up view of a scoop attached at one front float. For the considered heaviest mass configuration, the model floated at a pitch angle of 8.5 deg and a roll angle of 1.8 deg.

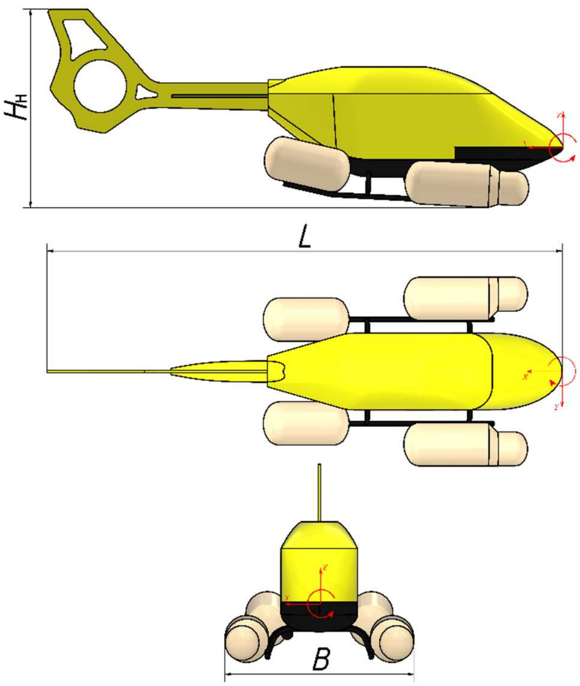

(a)

(b)

Figure 1: Drawing of the helicopter model including the model-fixed coordinate system (a), and close-up view of one front float equipped with a scoop (b)

The CoG and moment of inertia were adjusted by placing lead weights inside the model. The model's CoG differed by about 0.5 mm, 0.3 mm, and 3.5 mm from its corresponding full-scale CoG in the *x*-, y-, and *z*-directions, respectively. The dry weight of the model was only 0.03% higher than the corresponding full-scale helicopter weight.

The model's moments of inertia were measured using a self-made rotating pendulum. The moment of inertia *I* was based on solving Eq. (1) to determine the oscillating period T_O and the torsional coefficient D^* of the coil spring used. The period T_O was evaluated by fitting the parameters ***a***, *b*, and ***c*** of an Eulerian function (Eq. (2)) covering four successive periods of the decaying oscillation. The angles ***α*** of the rotating oscillation were measured using an incremental encoder. Figure 2 presents the time histories of the measured oscillations and the fitted Eulerian function. Using this method, the combined inertia of the pendulum and the helicopter model were measured. Subtracting the inertia of the pendulum from the combined inertia of the pendulum and the model obtained the inertia of the helicopter model itself.

(1) $$I = \frac{T \cdot D^*}{4\pi^2}$$

(2) $$\alpha = a \cdot \sin(b \cdot T_O) \cdot e^{-T_O/c}$$

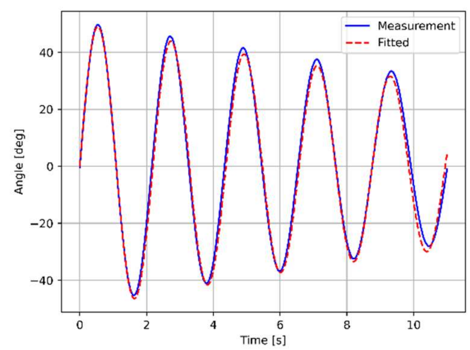

Figure 2: Time histories of the decaying oscillation of the rotating pendulum and the fitted Eulerian function

The resulting moments of inertia I_{xx} about the *x*-axis, I_{yy} about the *y*-axis, and I_{zz} about the ***z***-axis differed by only -5.9%, -6.6%, and 43.7%, respectively, from comparable full-scale inertias. (Negative deviations represent inertias lower than full-scale inertias.) The EASA (Ref. 11) specifications allow a margin of 10% for inertia modeling. The moment of inertia I_{zz} turned out to be significantly higher than allowed. However, I_{zz} had only a minor influence on the helicopter's floating stability because, according to Kidwell and Crago (Ref. 12), the helicopter is likely to capsize only about its longitudinal axis, i.e., the *x*-axis. The helicopter model was equipped with an Inertial Measurement

UNIT (IMU), type Lord 3DM-GX5-25, and a Bluetooth-adapter to transfer the measurements wirelessly to a computer. The IMU measured rotational angles and translational accelerations in six degrees-of-freedom (DoF) at a sampling rate of 100 Hz. The IMU and the Bluetooth-adapter were wrapped in a zip-bag to protect them from water ingress. Distances in the *x*-, *y*-, and *z*-directions between the helicopter's CoG and the IMU's measurement point were $0.062L$, $-0.02B$, and $0{,}1H_H$, respectively. The model-fixed coordinate system specified positive pitch angles when the nose moved upwards; roll angles, when the portside moved upwards; yaw angles, when the model turned to starboard. A yaw angle of 0 deg defined the model in head waves. The model-fixed coordinate system is also depicted in Graph (a) of Figure 1. Table 1 lists normalized particulars of the model.

Table 1: Normalized model particulars

L/B	2.89
L/H_H	2.58
X_{CoG}/L	0.31
Y_{CoG}/B	0.02
Z_{CoG}/H_H	0.13
$I_{XX}/(mBH_H)$	0.048
$I_{YY}/(mLH_H)$	0.061
$I_{ZZ}/(mLB)$	0.083

2.2. THE WAVE BASIN

The experiments were carried out in the deep-water towing tank of the Technical University of Berlin. The basin has a length of 250 m, a width of 8.1 m, a maximum water depth of 4.3 m, and it is equipped with a flap-type wave generator, which actively dampens incoming waves. Passive beaches placed at the far end of the basin reduce wave reflections.

The basin was equipped with eight parallel analog ultrasonic wave gauges to measure water surface displacements. Each wave gauge had a length of 700 mm and measured the surface elevation at a sampling rate of up to 128 Hz. As the wave gauge lengths were insufficient to capture the highest waves, their immersion depth was varied to record high wave crests and low wave troughs. By combining the signals of two wave gauges, all waves were fully captured. The wave gauges were placed in front of the test section at a distance of 29.3 m from the wave generator. Figure 3 shows a typical arrangement of the wave gauges situated in the cross-sectional shape of the wave basin. All dimensions are in millimeters, and the view is in the wave direction. This figure shows also location of the global X', Y, Z' coordinate system.

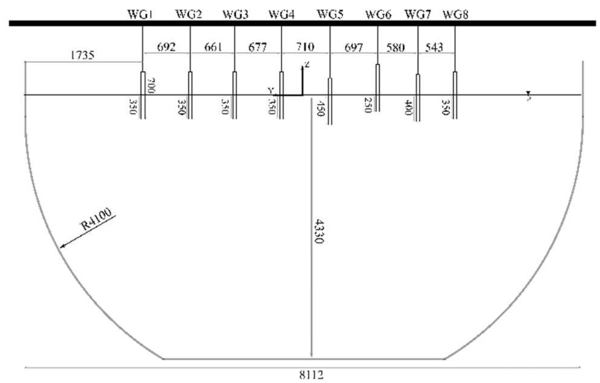

Figure 3: Arrangement of wave gauges situated in the cross-sectional shape of the wave basin. All dimensions are in millimeters.

Three ultrasonic wave probes, type General Acoustics UltraLab having a measurement range of 1300 mm, measured the water surface elevations around the helicopter model. Two wave probes were placed 2.5 m in front of the initial position of the helicopter model, with a distance of 0.4 m between them. The third wave probe was mounted 1.5 m at the model`s portside. All three wave probes were mounted on the towing carriage. When the model drifted during an experiment, the towing carriage was manually moved along with moving model. Thus, the distance between wave probes and helicopter model changed during a test run. A HBM QuantumX data acquisition system recorded the sensor signals at 100 Hz sampling rate. Figure 4 pictures the initial test setup before the start of wave generation and specifies the arrangement of the ultrasonic wave probes. This figure shows also the location of the global X', Y', Z' coordinate system.

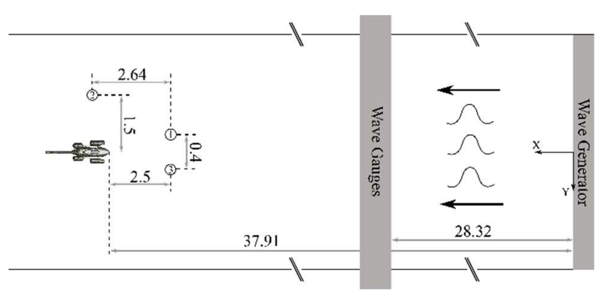

Figure 4: Experimental setup before the start of a test run and the arrangement of the ultrasonic wave probes. All dimensions are in meters.

2.3. WAVE MODELING

The JONSWAP spectrum (Ref. 20) modeled the sea states as long-crested irregular waves. Equations (3), (4), and (5) defined a seaway's spectral density, where H_S is the significant wave height, ω_P is the circular peak frequency, ω is the circular frequency, and γ is the peak enhancement factor, here set as 3.3.

$$S(\omega) = \frac{5}{16}\omega_P H_S^2 \omega^{-5} \cdot \exp\left(-\frac{5}{4}\left(\frac{\omega}{\omega_P}\right)^{-4}\right)\gamma^r \cdot (1 - 0.287 \cdot \log(\gamma)) \tag{3}$$

$$r = \exp\left(-0.5\left(\frac{\omega - \omega_P}{\sigma\omega_P}\right)^2\right) \tag{4}$$

$$\sigma = \begin{cases} 0.07 \text{ for } \omega \le \omega_P \\ 0.09 \text{ for } \omega > \omega_P \end{cases} \tag{5}$$

Although only 1.4% of all helicopter losses occurred in a sea state 6 (Ref. 2), for most offshore operations, a significant wave height of 6 m represents the most severe operational condition. Thus, we considered H_S = 6 m and T_Z = 7.9 s as well as H_S = 5 m and T_Z = 7.3 s for comparison. The significant wave height H_S and the zero-crossing period T_Z represented full-scale seaways taken from Ref. 11. Recall that, for a JONSWAP spectrum of γ = 3.3, the zero-crossing period T_Z is equal to the peak period T_P divided by 1.29.

2.4. TEST PROCEDURE

To evaluate a helicopter's floating stability, EASA recommend studying the capsize probability of a helicopter floating in a certain sea condition. For a helicopter equipped with intact floats, the capsize probability must be less than 3% and less than 30% when one float is damaged. Equation (6) determined the capsize probability P_{capsize}, based on the test duration T_{Test}, the time intended to evacuate the helicopter after ditching $T_{\text{criterion}}$ = 5 min (full-scale), and the number of capsize events N_{capsize}. Equation (7) determined the test duration T_{Test}, based on the resulting maximum allowed capsize probability $P_{\text{capsize,max}}$, the test criterion $T_{\text{criterion}}$, and the required confidence level of C = 95%. Thus, the full-scale test duration for a helicopter with intact floats was 499 min, which represented the model-scale test duration of 144.13 min.

$$P_{\text{capsize}} = \frac{N_{\text{capsize}} \cdot T_{\text{criterion}}}{T_{\text{test}}} \tag{6}$$

$$T_{\text{Test}} = -\frac{T_{\text{criterion}} \cdot \ln(1 - C)}{P_{\text{capsize,max}}} \tag{7}$$

As the reflected waves at the basin's ends altered the wave spectrum, we subdivided our floating stability tests into sections of 3.0 min duration. Each test run consisted of a wave generation lasting for 3.5 min. The first thirty seconds were treated as a fade-in period because smaller waves required more time to reach the model, and the remaining three minutes were then analyzed to evaluate the helicopter's floating stability.

At the beginning of each test run, the helicopter model, with a yaw angle of 0 deg, was manually placed about 37.9 m behind the wave generator, as shown in Figure 4. The model was not moored and, thus, it was free to move in all six DoFs. The model moved less than 20 m in the X'-direction and about ±2 m in the Y'-direction.

To evaluate the helicopter's floating stability, different configurations had to be considered. The mass configurations representing the lightest and heaviest load conditions were analyzed. Additionally, intact and damaged floating conditions had to be considered. For the damaged condition, the buoyancy of one compartment of one float was neglected, and then the missing buoyancy was most severe. However, intact floats combined with the heaviest mass configuration represented the most stable floating conditions. Thus, when the capsize probability for this case was higher than allowed, we considered the other helicopter configurations to be obsolete. Additionally, we accounted for the case of one open passenger door during flotation. This case could occur when ditching becomes necessary during lifting operations at low altitude. The ingress of water entering the helicopter may also reduce the floating stability of the ditched helicopter.

3. RESULTS

The analysis of the experiments focusses on five objectives. Firstly, the quality of the modeled waves is analyzed. Secondly, the upright flotation behavior of the helicopter floating in waves of a significant wave height of 5 and 6 m is evaluated. Next, the repeatability of the experiments is studied. Fourthly, the influence of different helicopter configurations was analyzed. Here, the influence of one opened door and attached scoops is addressed. The last section studies capsize events and quantifies capsize probabilities, which was the main objective of the test campaign. Thus, some tests were carried out without active IMU influencing the analyzed test durations. Additionally, some conditions were tested for a shorter test duration due to a limited total test duration.

3.1. WAVE SPECTRA AND WAVE PROPERTIES

For a free-floating model, the measured wave spectrum must match the modeled spectrum over the complete test section length. Here, the test section had a length of 20 m. Thus, the wave spectrum of the same draw of a wave train having a significant eave height of 6 m was measured using the wave gauges in steps of 5 m inside the test section. Additionally, waves were measured in front of the test section where the wave gauges are placed during flotation stability tests. Figure 5 plots the spectra measured at all positions showing only minor differences between the spectra. These differences may result from the repeatability accuracy of the wave generator. Also, the differences between spectra are larger for longer waves, which indicates that there might be reflected waves remaining from previous tests inside the basin. However, the small differences show that measured wave spectra in front of the test sections are valid for the complete test section.

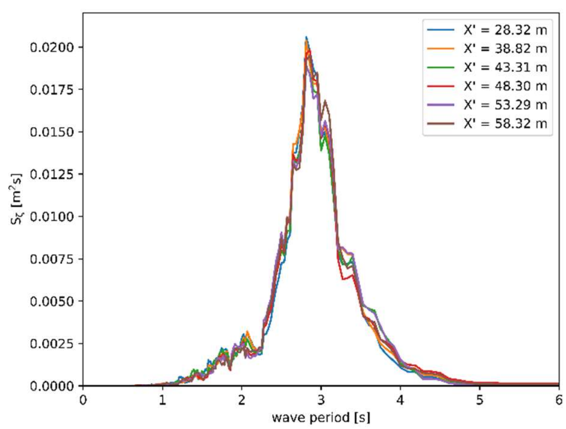

Figure 5: Wave spectra measured at different position within and in front of the test section

Figure 6 shows the time histories of the water surface elevation measured at three parallel wave gauges. For a long-crested seas, the time histories should match. Here, the signals of the two wave gauges 1 and 8, located close to the tank walls, match favorably. Wave gauge 4, located in the tank center, shows slightly lower wave troughs and slightly higher wave crests. However, the small differences indicate the long-crestedness character of the modeled sea.

Figure 7 considers the distribution of wave amplitudes occurring for significant wave heights of 5 and 6 m. For both conditions, the median and maximum measured wave amplitudes were 136.5 and 459.0 mm, and 169.5 and 505.1 mm, respectively.

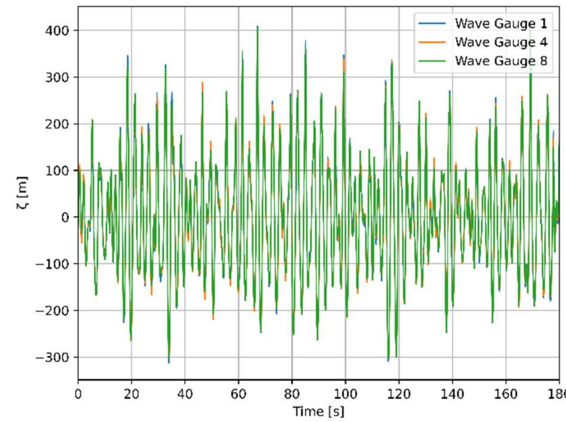

Figure 6: Water surface elevations measured at three parallel wave gauges

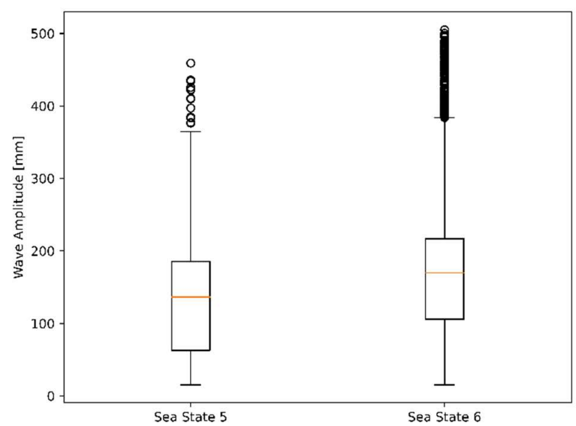

Figure 7: Distribution of wave amplitudes for measurement periods of 9371 s and 3900 s for H_S = 6 and 5 m, respectively

Figure 8 depicts the exceedance probabilities of wave amplitudes for significant wave heights of 5 and 6 m for the considered measurement durations of 3900 and 9371 s, respectively. The related wave amplitudes at exceedance probabilities of 1 and 0.1% for significant wave heights of 5 and 6 m were 308.4 and 384.6 mm, and 357.6 and 456.7 mm, respectively. These statistic reference values characteries the sea conditions and might be used for future designs of helicopters and helicopter equipment.

The measured sea spectra resulting from all draws were compared with the reference spectra to quantify the suitability of the modeled waves. Figure 9 compares the measured sea spectra of the different helicopter configurations with the reference spectrum for a significant wave height of 6 m as well as the measured spectrum and reference spectrum for a significant wave height of 5 m. Minor differences indicate the suitability of the modeled waves. These small differences resulted from the non-infinite test duration.

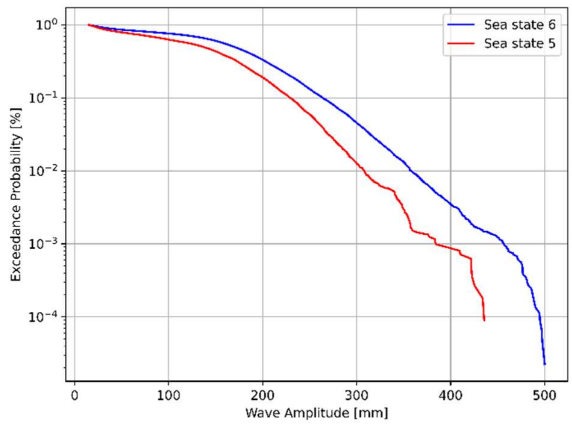

Figure 8: Exceedance probabilities of wave amplitudes for a measurement period of 9371 s and 3900 s for H_S = 6 and 5 m, respectively

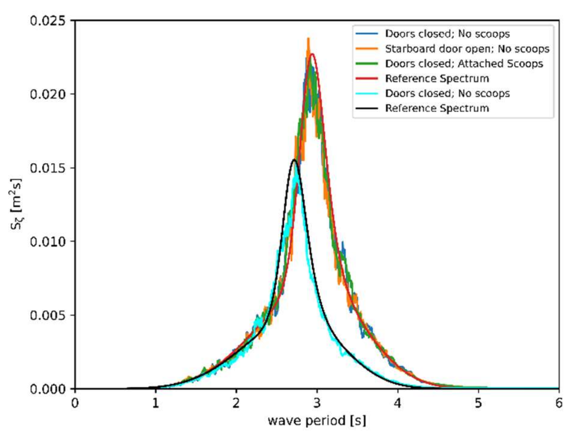

Figure 9: Measured sea spectra of the three helicopter configurations and the reference sea spectra representing H_S = 5 m (black) and H_S = 6 m (red)

To quantify the differences between measured and reference spectra, the area below the spectrum curves and corresponding H_s of the measured spectrum and the reference spectrum were compared. For a significant wave height of 6 m, the differences of the area below measured and reference spectrum in the range of wave periods between 0 and 6 s were between 3.51 and 0.81% for the three helicopter configurations; for a significant wave height of 5 m the difference was 6.12%. The higher difference for H_S = 5 m resulted from the shorter test period compared to H_S = 6 m. The differences between the significant wave height of the measured waves and the reference spectra were between 1.82 and 0.59% for predefined H_S = 6 m and 3.85% for predefined H_S = 5 m. This empathizes that the model seas matched the defined test cases favorably.

3.2. FLOTATION BEHAVIOR FOR SIGNIFICANT WAVE HEIGHTS OF 5 AND 6 METERS

To understand the results of the analyzed helicopter motions, the general process of a single test run must be understood. When starting the wave generation, longer waves travel faster than shorter waves. Thus, long regular wave arrived at the helicopter first. Consequently, the model starts pitching and yaws about 90 deg. Due to the model yaw motion, model's pitch motions decrease and roll motions increase. This explains why pitch motions are predominantly small and roll motions dominate model motions. However, in single test runs the yaw angle stays around 0 deg for a longer time, which can alter exceedance probability plots significantly. After 30 seconds the shortest waves arrived at the model and the sea is completely developed. The subsequent 180 seconds are used to analyze the flotation behavior. Figure 10 plots the time histories of the roll, pitch and yaw angle of one test run. Here, at time instance zero the first wave arrived at the model. For the study of flotation stabilities, the analysis was split in two parts: Firstly, flotation without capsizing and, secondly, capsizing events.

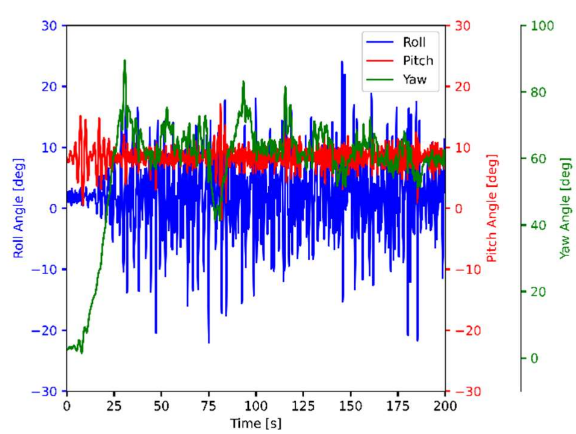

Figure 10: Time histories of roll, pitch, and yaw angle of a typical test run

Figure 11 depicts the exceedance probabilities of roll, pitch and heave amplitudes as well as vertical and lateral acceleration amplitudes measured for a significant wave height of 6 m over a duration of 8448 seconds for a helicopter with closed doors and no scoops. Heave motions were calculated from the acceleration signals through two-fold integration. Especially the roll motions and accelerations influence the conditions for evacuating a helicopter after ditching. The resulting amplitudes at exceedance probabilities of 1 and 0.1% were 22.4 and 28.0 deg for roll motions, 12.4 and 18.2 deg for pitch motions, 394.4 and 485.9 mm for heave motions, 3.4 and 5.2 m/s^2 for vertical accelerations, and 2.9 and 4.9 m/s^2 for lateral accelerations (model-fixed *Y* direction).

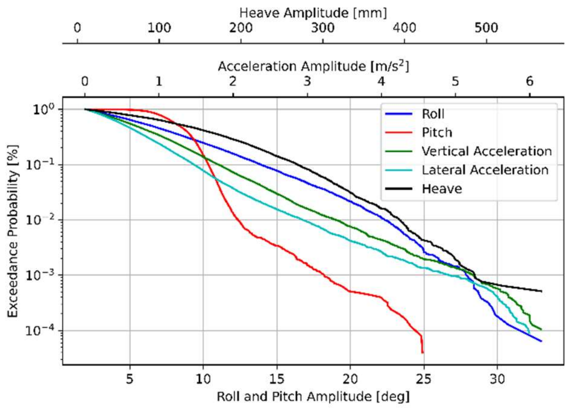

Figure 11: Exceedance probabilities of roll, pitch, and heave and vertical and lateral acceleration amplitudes for the helicopter with closed doors and with floats without scoops for a test duration of 8448 s for H_S = 6 m

The exceedance probabilities of roll, pitch, heave, as well as vertical and lateral acceleration amplitudes for a significant wave height of 5 m are shown in Figure 12. Here, the considered test duration was 3416 seconds. The resulting amplitudes at exceedance probabilities of 1 and 0.1% were 20.6 and 27.8 deg for roll motions, 12.7 and 19.3 deg for pitch motions, 338.8 and 466.0 mm for heave motions, 3.1 and 4.2 m/s^2 for vertical accelerations, and 2.6 and 4.2 m/s^2 for lateral accelerations.

Figure 13 directly compares roll amplitudes resulting for significant wave heights of 5 and 6 m. Here, the trends of the exceedance probabilities are similar while roll angles for H_S = 5 m are smaller than for H_S = 6 m. However, at an exceedance probability of 1% the difference was 8%. For pitch motions the difference between significant wave heights of 5 and 6 m at an exceedance probability of 1% was only 2.4% while the difference of heave amplitude was 14.1%. Consequently, the small change of peak period has only a minor effect on roll amplitudes, but the change of wave height significantly influences heave motions.

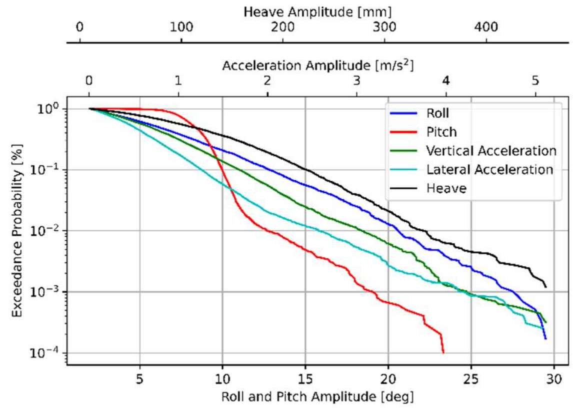

Figure 12: Exceedance Probabilities of roll, pitch, and heave and vertical and lateral acceleration amplitudes for the helicopter with closed doors and with floats without scoops for a test duration of 3416 s for H_S = 5 m

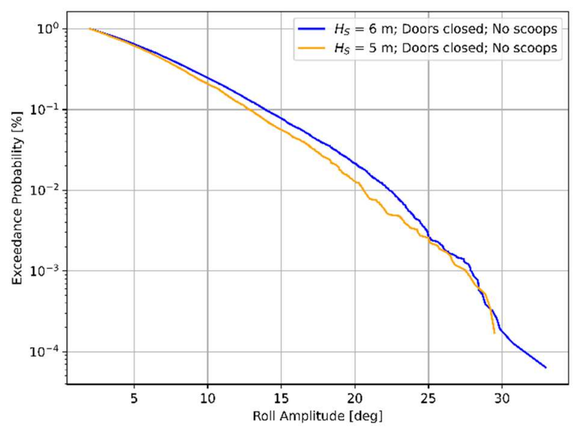

Figure 13: Exceedance probabilities of roll amplitudes for H_S = 5 and 6 m

3.3. REPEATABILITY

The quantification of repeatability is crucial to evaluate if differences of measured helicopter motions for varying configurations result from the configuration itself or from a variation of waves. Therefore, one draw having a significant wave height of 6 m was tested two times. Graph (a) of Figure 14 shows the time histories of the water surface elevations, which match favorably. Single peaks differed slightly having a difference of maximum 25 mm. Graph (b) pictures resulting yaw motions of a helicopter floating in the waves shown in graph (a). The general trend of yaw angles is similar for both repetitions. The model oscillated around an angle of 65 deg but yawed to approximately 40 deg around the time instance of 40 seconds. However, the yaw angles sometimes differed up to 20 deg.

Recall that the main objective of the flotation stability studies was the quantification of capsize probabilities. Thus, the repeatability of capsize events determined the repeatability of the experiments. Graph (c) of Figure 14 plots the time histories of roll and pitch motions of both repetitions. The repetitions match favorably showing only minor differences. At time instance of 178 seconds the helicopter capsized, and roll angles increased rapidly for both test runs. Additionally, pitch angles decreased synchronously. The capsizing happens at the same time instance for both test runs, which empathizes the good repeatability of the experiments. Capsize events as well as the process leading to capsizing are analyzed in section 3.5.

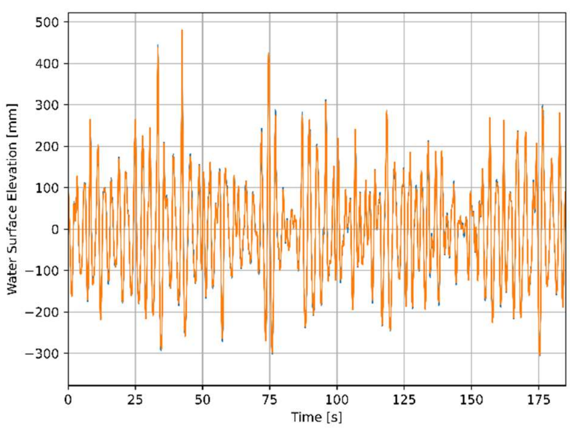

(a)

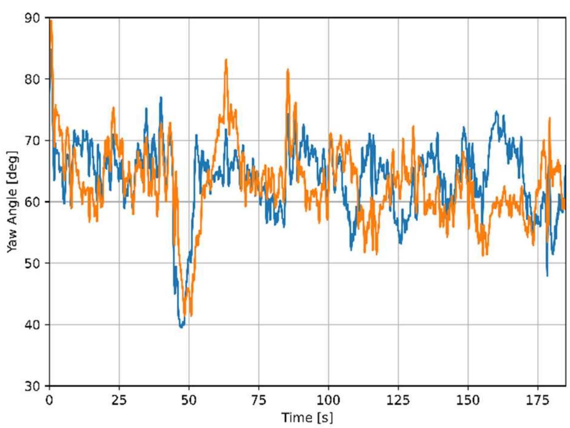

(b)

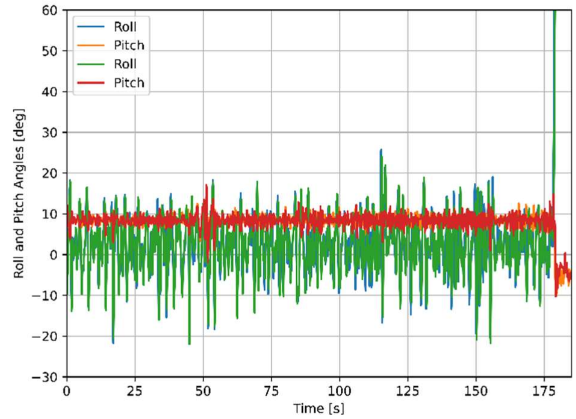

(c)

Figure 14: Time histories of water surface elevations (a), helicopter yaw angles (b), and helicopter pitch and roll angles (c) of two representative repetitions of the same test runs

3.4. COMPARATIVE HELICOPTER CONFIGURATIONS

This section considers the flotation behavior of helicopter having closed doors and no scoops, one opened door and no scoops, and closed doors and attached scoops. For all tests, the floats are intact, and the helicopter is ballasted according to the heaviest load configuration. To identify influences of the three configurations, only draws were considered where the motion and wave measurement worked properly for all helicopter configurations. The considered test duration was 3882 seconds for the helicopter with closed doors and without scoops, 3988 seconds with the starboard door opened and without scoops, and 4144 seconds for the helicopter with closed doors and attached scoops.

Figure 15 compares exceedance probabilities of roll amplitudes for the three configurations. The trends of all configurations were similar. The opened door had no effect on resulting roll amplitudes while the application of scoops increased roll amplitudes. The roll amplitudes at 1% exceedance probability were 22.19 deg (doors closed; no scoops), 22.23 deg (one door opened; no scoops), and 23.27 deg (doors closed, scoops attached).

Figure 16 plots the distribution of roll amplitudes for the three helicopter configurations. Median roll amplitudes were 6.52, 6.42 and 7.33 deg, while the 90%-quantile were 13.97, 13.94 and 14.99 deg, respectively. This emphasizes that one opened door had no influence on roll amplitudes, but the utilized scoops increased roll amplitudes. Scoops increased the median roll amplitude about 11.05%, and the roll amplitude at 1% exceedance probability about 4.64%. This is surprising because scoops are usually applied to increase the flotation stability.

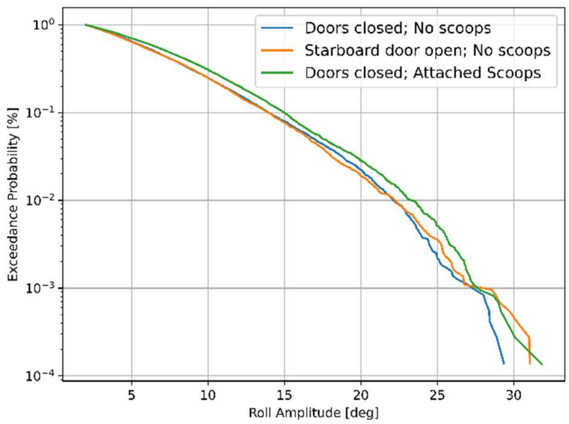

Figure 15: Exceedance probabilities of roll amplitudes for three helicopter configurations for H_S = 6 m

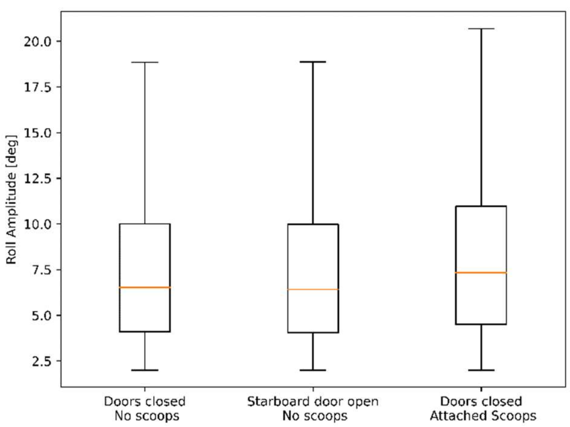

Figure 16: Distribution of roll amplitudes for three helicopter configurations for H_S = 6 m

Exceedance probabilities of pitch amplitudes are pictured in Figure 17. At 1% exceedance probability pitch amplitudes were 12.07, 13.38 and 12.78 deg, respectively. The differences might result from the manual model alignment at the start of each test run. If the model was perfectly aligned at the start of a test run (yaw angle of 0 deg), the model kept its heading for a longer time yielding higher pitch angles.

Exceedance probabilities of heave amplitudes are depicted in Figure 18. At exceedance probabilities of 1% heave amplitudes were 387.3, 400.1, 414.3 mm, respectively. The difference of 27 mm was in the magnitude of the wave generation repeatability. Thus, the differences resulted from the repetitions and not from the considered helicopter configurations.

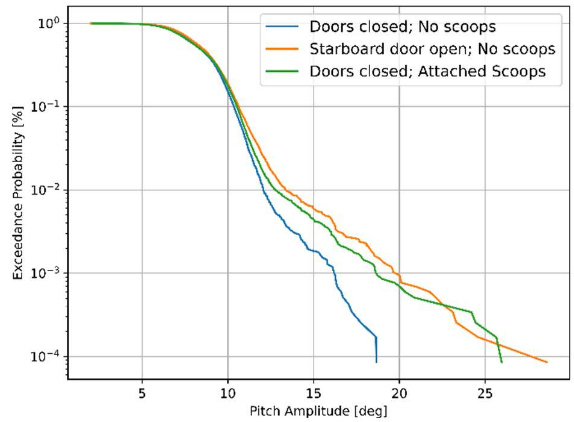

Figure 17: Exceedance probabilities of pitch amplitudes for three helicopter configurations for H_S = 6 m

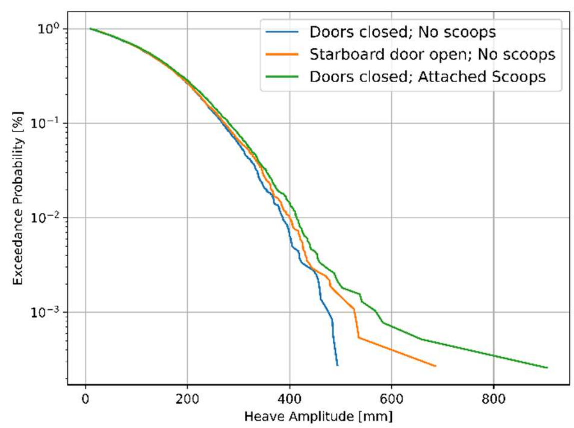

Figure 18: Exceedance probabilities of heave amplitudes for three helicopter configurations for H_S = 6 m

Figure 19 plots related exceedance probabilities of acceleration amplitudes. At 1% exceedance probability vertical acceleration amplitudes were 3.46, 3.23 and 3.18 m/s^2, respectively, and lateral acceleration amplitudes were 3.23, 2.97 and 3.64 m/s^2, respectively. The small differences between the helicopter configuration again resulted from the repeatability accuracy.

3.5. CAPSIZE EVENTS

This section addresses the capsizing events captured for significant wave heights of 5 and, predominately, 6 m. To visualize the capsizing process, we need to consider helicopter's yaw and roll angles as well as the wave properties during capsizing. Therefore, we consider capsizing events happened for the helicopter (closed doors; no scoops) floating at H_S = 6 m.

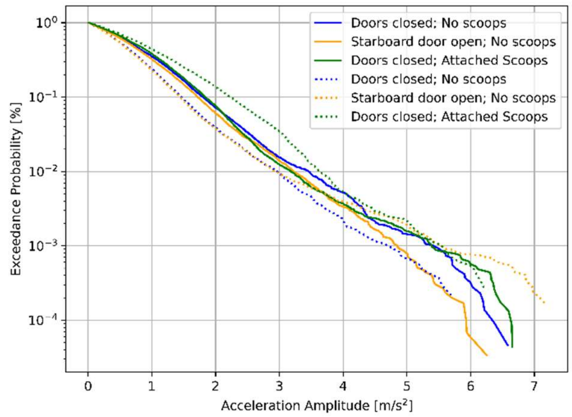

Figure 19: Exceedance probabilities of vertical acceleration amplitudes (continuous lines) and lateral acceleration amplitudes (dashed lines) for three helicopter configurations for H_S = 6 m

Figure 20 plots time histories of yaw angles of 13 capsizing events. Here, the helicopter always yawed about ≈90 deg before capsizing. The yaw direction depended on the initial angle of the model. Recall that the model was aligned manually before each test. The turning process usually takes less then 40 seconds. However, for two test runs the helicopter model remained in its initial position for a longer duration. In both cases the initial angle was smaller compared to the residual test runs. Consequently, the encounter angle between helicopter and waves during capsizing was between 50 and 120 deg.

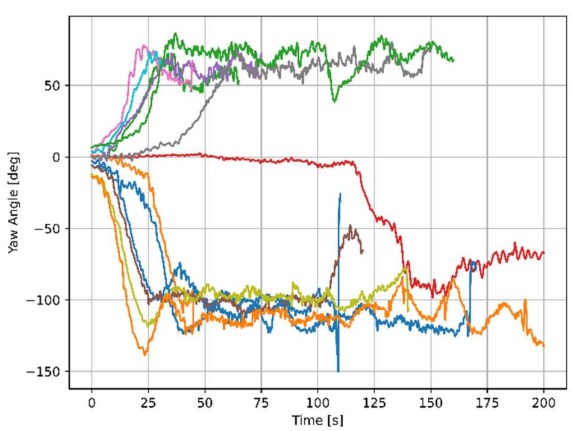

Figure 20: Time histories of yaw angle during capsizing for H_S = 6 m

Figure 21 shows the time histories of roll angles corresponding to yaw motions plotted in Figure 20. The roll angle time histories usually oscillated up to an amplitude of 25 deg. There are no signs announcing capsizing. Capsizing occurred suddenly having a rise time (from 0 to 70 deg roll angle) between 0.74 and 1.98 seconds. The direction of capsizing depends on the model's yaw direction. Consequently, the helicopter always capsized about its roll-axis when it was floating in beam waves.

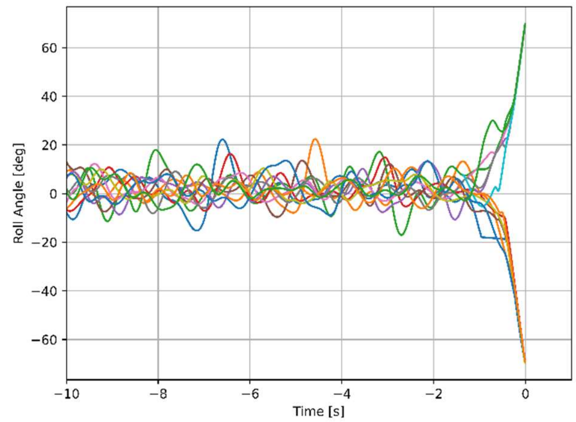

Figure 21: Time histories of roll angle during capsizing for H_S = 6 m

To analyze which condition yield capsizing, Figure 22 depicts the change of water surface elevations ζ of five exemplary test runs measured at wave probe 2. At the moment of capsizing (time instance zero) a steep wave arrived, broke and hit the helicopter. Recall, that the towing carriage carrying the wave probe was manually controlled. Thus, there was a varying distance between wave probe and model which caused the time shift between capsize event and occurrence of the steep wave displayed in Figure 22. Summarizing, capsizing only happened if a breaking wave hit the helicopter floating in beam waves.

To address the capsize probability the number of capsize events and the test duration were considered for four test cases, namely helicopter with closed doors and without scoops at H_S = 5 m, helicopter with closed doors and without scoops at H_S = 6 m, helicopter having an open starboard door and no scoops at H_S = 6 m, and helicopter with closed doors and equipped with scoops at H_S = 6 m. For H_S = 6 m the test duration for the three helicopter configurations were 162.2 minutes, 153.6 minutes, and 88.0 minutes, respectively. In this time thirteen, nine, and eight capsize events happened, respectively, yielding a capsize probability of 11.57, 8.45, and 13.12%, respectively. For H_S = 5 m one helicopter configuration was tested for 65.5 minutes, where 3 capsize events happened yielding a capsize probability of 6,61%. Table 2 summarizes the determined capsize probabilities.

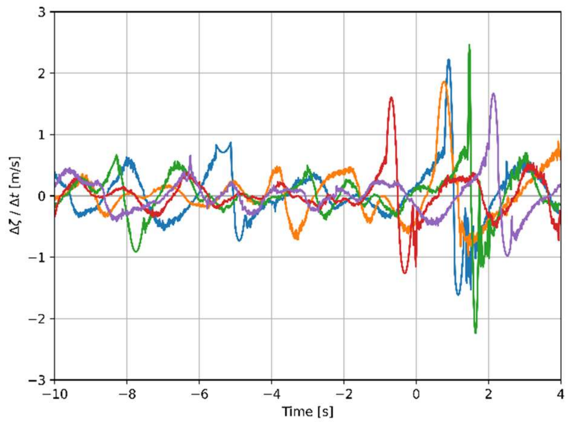

Figure 22: Rate of wave amplitude change during capsizing measured at wave gauge 2 for H_S = 6 m

Table 2: Capsize probabilities

H_S	Door configuration	Scoops	Capsize probability
5	Both closed	None	6.61%
6	Both closed	None	11.57%
6	Both closed	Yes	13.12%
6	Starboard door open	None	8.45%

The observations lead to the conclusion that none of the test conditions is closed to fulfilling the criterions specified by EASA to approve a certification. Here, a 3% capsize probability is allowed. For H_S = 6 m, the attachment of scoops has no positive effect on the capsize probability. Contrary, the capsize probability with scoops is 1.55% higher than without scoops. However, the test duration with scoops was only 88 minutes of the required 144.1 minutes. Thus, the capsize probability might be slightly overpredicted. Our experience showed that only minor changes of capsize probability happened when more than 50% of the required tests duration was carried out. However, the test procedure is a statistical approach, and it is possible that all capsize events happen in some of the last test runs.

For the helicopter having one opened door, the capsize probability was reduced to 8.45%. This is surprising because opening one door had no influence on the exceedance probabilities of roll angle amplitudes. The difference resulted from a change of used draws between the testing of both helicopter configurations. However, this highlights the impact of draw selection of resulting capsize probabilities. Using or skipping certain draws might significantly alter capsize probabilities. If we only considered the draws which were identical for the three helicopter configurations (see section 3.4.), the capsize probability was 15.12, 12.67, and 15.51%, respectively. Here, the capsize probability was still lower for the configuration having one open door. However, for one opened door, the number of capsize event was only one events lower compared to both other helicopter configurations while the test duration is similar for all cases. Thus, opening one door has no significant effect on the capsize probability.

For a significant wave height of 5 m the capsize probability of a helicopter with closed doors and without scoops reduced to 6.61%. Here, the test duration was only 65.5 minutes, which is 45.4% of the required test duration. Thus, the probability might change slightly for a longer test duration. However, limiting helicopter operation to H_S = 5 m still does not significantly reduce the capsize probability.

4. CONCLUSIONS

In the present study, we examined the flotation stability of a modern light helicopter equipped with a state-of-the-art flotation system. Capsizing only happened if a breaking wave hit the helicopter in beam waves. The evaluated capsize probability of a helicopter with closed doors and without scoops was 15.12% for a significant wave height of 6 m and 6.61% for significant wave height of 5 m. Additional attachment of scoops did not decrease the capsize probability and was not suitable to increase flotation stability. This highlights the demand of new flotation system designs increasing flotation safety.

Additionally, wave properties, and helicopter heave, roll, pitch as well as vertical and lateral accelerations were analyzed statistically. These results are suitable for the validation of numerical simulations and for the design of new helicopters and helicopter equipment.

Author contacts:

Simon Tödter: simon.toedter@uni-due.de

Jens Neugebauer: jens.neugebauer@uni-due.de

Stefan Harms: stefan.harms@airbus.com

Ould el Moctar: ould.el-moctar@uni-due.de

Thomas E. Schellin: dr_thomas_schellin@yahoo.de

5. ACKNOWLEDGMENTS

This study was part of the research project EvoS-BraWa, funded by the Bavarian Ministry of Economic Affairs and the Regional Development and Energy (StMWi) of the Bavarian Aviation Research Program (BayLu25), under grant ROB-2-3410.20-04-10-36 / BLU-2109-0036.

We thank Prof. Andrés Cura-Hochbaum, Karsten Riek, Sebastian Sperling, and Aaron Lange for their support, effort, and craftsmanship during the experiments.

6. REFERENCES

1. Clifford, W. S., “Helicopter crashworthiness. Study I. A review of UK military and world civil helicopter water impacts over the period 1971-1992,” CAA Paper 96005. London: Civil Aviation Authority, 1996.

2. Downie, M., and Gosling, D., “Offshore helicopter travel: is the UK oil and gas industry failing offshore workers?,” *New solutions: a journal of environmental and occupational health policy,* Vol. 29, (4), 2020, pp. 504-518. DOI: 10.1177/1048291119887189.

3. Civil Aviation Authority, “Safety Review of Public Sector Transport Helicopter in Support of the exploitation of oil and gas,” CAP 1145, 2014.

4. Rowe, S. J., Howson, D., and Sparkes, P., “Research improving the safety of offshore helicopter operations,” Proceedings of 1st Offshore Technology Conference, Houston, Texas, U.S.A., 2002.

5. Aziz, A., Amir, M. A. U., Roshamida, A. J., Samsudheen, I., Sariff, E. S. M., Rahman, A., and Rosly, A., “Helicopter ditching incident analysis: Classification of risk factors,” *Journal of Engineering Science and Technology*, Vol. 18, (1), 2023, pp.113-122.

6. Federal Aviation Administration, “Rotorcraft ditchings and water-related impacts that occurred from 1982 to 1989 – Phase II,” DOT/FAA//CT-92/14, 1993.

7. Brooks, C. J., MacDonald, C. V., Donati, L., and Taber, M. J., “Civilian Helicopter Accidents into Water: Analysis of 46 Cases, 1979-2006,” *Aviation, Space, and Environmental Medicine*, Vol. 79, (10), pp. 935-940, 2008. DOI: 10.3357/ASEM.2247.2008.

8. Taber, M. J., and McCabe, J., “An examination of survival rates based on external flotation devices: A helicopter ditching review from 1971 to 2005,” *SAFE Journal*, Vol. 35, (1), pp. 1-6, 2007.

9. Reader, D. C., “Helicopter Ditchings - British Military Experience 1972-1988,” RAF IAM Report No 677, 1990.

10. European Union Aviation Safety Agency, “Certification Specifications and Acceptable Means of Compliance for Small Rotorcraft,” Technical Report, 2020.

11. European Union Aviation Safety Agency, “Certification Specifications and Acceptable Means of Compliance for Small Rotorcraft,” Certification specification CS-27, Amendment 9, Technical Report, 2020.

12. Kidwell, J. C., and Crago, W. A., “Model testing to establish ditching and flotation stability characteristics of a helicopter,” Proceedings of the 26th Annual National Forum of the American Helicopter Society, Washington D.C., U.S.A., 1970.

13. Wilson, F. T., and Tucker, R. C. S., “Ditching and Flotation Characteristics of the EH101 helicopter,” Proceedings of the 13th European Rotorcraft Forum, Arles, France, 1987.

14. Alcedo, A. M., “Design and testing of float landing gear systems for helicopters,” *Journal of the American Helicopter Society*, Vol. 25, (3), pp. 3-9, 1980.

15. Delorme, L., Denante, M., Santucci, P., and De Gelas, A., “New floatation devices to avoid helicopters’ total inversion after capsize,” Proceedings of the 10th International Conference on Stability of Ships and Ocean Vehicles, St. Petersburg, Russia, 2009.

16. Kraskowski, M., “Numerical and experimental analysis of the helicopters’ flotation system,” Proceedings of the 45th European Rotorcraft Forum, Warsaw, Poland, 2019.

17. Katsuno, E. T., Peters, A., Lantermann, U., Beham, A., Harms, S., and el Moctar, O., "Numerical simulations of helicopter ditching," Proceedings of the 24th Numerical Towing Tank Symposium, Zagreb, Croatia, 2022.

18. Katsuno, E T., Peters, A., and el Moctar, O., "Seakeeping Behavior of a Helicopter Landing in Waves," Proceedings of the 42nd International Conference on Ocean, Offshore and Arctic Engineering, Melbourne, Australia. 2023. DOI: 10.1115/OMAE2023-105235

19. Katsuno, E. T., Peters, A., and el Moctar, O., "Numerical Seakeeping Analysis for a Floating Helicopter after Ditching in Waters," Journal of Offshore Mechanics and Arctic Engineering, Vol. 147, (1), pp. 011401. DOI: 10.1115/1.4065709

20. Hasselmann, K., Barnett, T. P., Bouws, E., Carlson, H., Cartwright, D. E., Enke, K., Ewing, J. A., Gienapp, H., Hasselmann, D. E., Kruseman, P., Meerburg, A., Muller, P., Olbers, D. J., Richter, K., Sell, W., and Walden, H., “Measurements of wind-wave growth and swell decay during the Joint North Sea Wave Project (JONSWAP),” *Ergänzungsheft zur Deutschen Hydrographischen Zeitschrift Reihe*, Vol. 8, 12, pp. 95, 1973.